Tutor

Dra. Mercè Deumal Solé

Departament de ciència dels materials i química física. Secció de química física.

Grau de Química

Treball Final de Grau

Computational study of organic radicals of technological interest in molecule-based magnetism.
Estudio computacional de radicales orgánicos de interés tecnológico en magnetismo basado en moléculas.

Sergio Pablo García Carrillo

June 2017

Universitat de Barcelona

B:KC Barcelona Knowledge Campus
Campus d'Excel·lència Internacional

"- But what am I going to see?

- I don't know. In a certain sense, it depends on you."

Stanisław Lem - Solaris

To Dr. M. Deumal for her patience, understanding and help,
to Dr. J. Ribas and Dr. J. M. Bofill for showing me the world of computational chemistry,
to A. García, to whom I owe my passion for science,
to J. M. Prieto, D. C. Guerra, O. Sánchez and A. Gil for their unconditional support,
and to C. Cabezas, for being always there.

Thank you all for making this possible.

REPORT

CONTENTS

1. SUMMARY

A new magnetic crystal composed of an anthranol/anthroxyl unit has been synthesized and characterized.[1] The crystal, which is composed by anthroxyl radicals, appears to undergo a magnetic phase transition when it reaches a temperature of *ca.* 100 K.

The anthranol/anthroxyl pairs found in the 100 K and 200 K structures (see *Figure I*) characterized by X-rays, show large differences in the position of the central hydrogen between the two oxygens in each pair. While in the structure at 100 K the hydrogen is bonded to the oxygen of the anthranol molecule, in the structure at 200 K the hydrogen seems to be delocalized between the two oxygens of the pair, thus forming two semi-radicals. Upon phase transition, a proton coupled electron transfer (PCET) reaction takes place.

(a) (b)

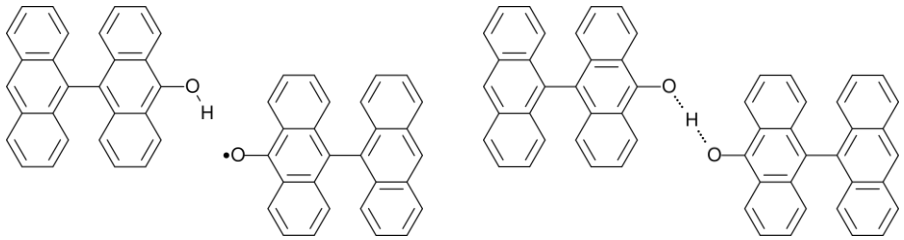

Figure I. Anthranol/Anthroxyl pair schematic structures. (a): structure at 100K, (b): structure at 200K

This work performs a computational study on the PCET reaction taking place inside the crystal as well as the topological changes leading the magnetic transition that occurs at *ca.* 100 K.

The study of the reaction is carried out in the gas phase through different anthranol/anthroxyl pairs extracted from the X-Ray crystal data. A study of the energies, the topology and the differences between the anthranol/anthroxyl pairs in the gas phase, as well as a search of the transition state for a better understanding of the reaction in the crystal is carried out.

The energy barrier for the proton coupled electron transfer (PCET) in gas phase has found to be 11.11 kcal mol^{-1}. It is believed that accounting for the anthranol/anthroxyl solid state environment would lead to a decrease of this barrier.

For a better characterization of the magnetic behavior of the system, a study of the distribution of spin density on both structures *Figure I (a) and (b)*, is performed, in which the semi-radical nature of the 200 K structure can be observed.

To carry out the magnetic analysis, different pairs of anthranol/anthroxyl dimers extracted from the two X-ray diffraction structures, at 100 K and 200 K, will be used. The magnetic coupling interaction of these dimers is calculated to be able to build the magnetic topology of the crystal. Once known, magnetic models are used to calculate the magnetic susceptibility of both structures and compare them with the value obtained experimentally.

The results obtained suggest that the structure at 100 K behaves diamagnetically. At 200 K, however, a dynamic behavior is observed since the structure found experimentally could be a statistical average of a set of structures belonging to the reaction path.

Finally, we have investigated whether electron-donor or withdrawing substituents can give rise to new anthranol/anthroxyl pairs with enhanced proton coupled electron transfer capabilities.

Keywords: PCET reaction, anthroxyl radical, anthranol, magnetic phase transition

2. RESUMEN

Se ha sintetizado y caracterizado un nuevo cristal magnético compuesto por unidades de antranol/antroxilo.[1] El cristal, que está compuesto por radicales antroxilo, parece sufrir una transición de fase magnética cuando alcanza una temperatura de *ca.* 100 K.

Los pares de antranol/antroxilo encontrados en las estructuras de 100 K y 200 K (ver *Figura I*) caracterizadas por rayos X, muestran grandes diferencias en la posición del hidrógeno central que se encuentra entre los dos oxígenos en cada par. Mientras que en la estructura a 100 K el hidrógeno está unido al oxígeno de la molécula de antranol, en la estructura a 200 K el hidrógeno parece estar deslocalizado entre los dos oxígenos del par, formando así dos semi-radicales. Tras la transición de fase, tiene lugar una reacción del tipo "*proton coupled electron transfer*" (PCET).

(a) (b)

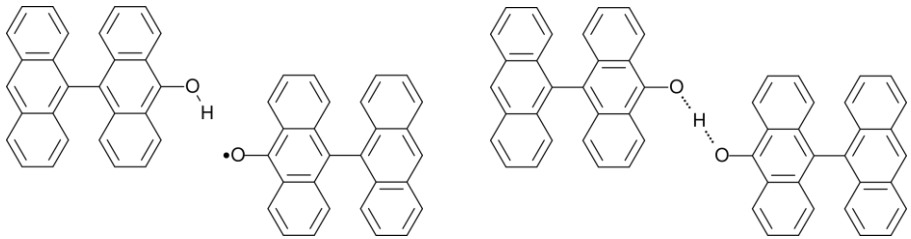

Figura I. Estructuras esquemáticas del par antranol/antroxilo A): estructura a 100 K, B): estructura a 200 K

Este trabajo realiza un estudio computacional de la reacción de PCET que tiene lugar dentro del cristal, así como los cambios topológicos que llevan a la transición magnética que se produce a *ca.* 100 K.

El estudio de la reacción se lleva a cabo fase gas a través de diferentes pares de antranol/antroxilo extraídos de los datos de la determinación por rayos X del cristal. Se realiza un estudio de las energías, la topología y las diferencias entre los pares de antranol/antroxilo en

fase gas, así como una búsqueda del estado de transición para una mejor comprensión de la reacción que tiene lugar dentro del cristal.

La barrera de energía para la reacción PCET en fase gas es de 11,11 kcal mol^{-1}. Se cree que teniendo en cuenta el entorno del sólido de antranol/antroxilo esta barrera de energía podría disminuir.

Para una mejor caracterización del comportamiento magnético del sistema, se realiza un estudio de la distribución de la densidad de spin en ambas estructuras de la *Figura I (a) y (b)*, en el que se puede determinar la naturaleza semiradicalaria de la estructura de 200 K.

Para llevar a cabo el análisis magnético, se utilizarán diferentes pares de dímeros de antranol/antroxilo extraídos de las dos estructuras, a 100 K y 200 K, caracterizadas por difracción de rayos X. La interacción del acoplamiento magnético de estos dímeros se calcula para poder construir la topología magnética del cristal. Una vez planteados, los modelos magnéticos se utilizan para calcular la susceptibilidad magnética de ambas estructuras y compararlas con el valor obtenido experimentalmente.

Los resultados obtenidos sugieren que la estructura a 100 K se comporta diamagnéticamente. A 200 K, sin embargo, se observa un comportamiento dinámico debido a que la estructura encontrada experimentalmente podría ser un promedio estadístico de un conjunto de estructuras pertenecientes al camino de reacción.

Finalmente, hemos investigado si los sustituyentes donadores o aceptores de electrones pueden dar lugar a nuevos pares de antranol/antroxilo que mejoren la reacción PCET.

Palabras clave: reacción PCET, radical antroxilo, anthranol, transición de fase magnética

3. INTRODUCTION

3.1. HAT AND PCET REACTIONS

Electron transfer (ET) and proton transfer (PT) reactions are two of the most important processes in chemistry. They are present in both organic and biological processes as well as in inorganic chemistry. There are some reactions that include both processes, an electron transfer and a proton transfer coupled together, namely hydrogen atom transfer (HAT) and proton coupled electron transfer (PCET) reactions.

Proton coupled electron transfer (PCET) reactions are a family of reactions that involve an electron and a proton transfer.[2] By definition these reactions are concerted and have no intermediate. Both the proton and the electron start from different orbitals and are transferred to different orbitals. These reactions typically involve different donors and a significant change in the charge distribution of the molecule. Such reactions play an important role in a wide range of chemical and biological processes, including photosystem II (see *Figure 1*),[3] respiration and enzyme reactions.[4]

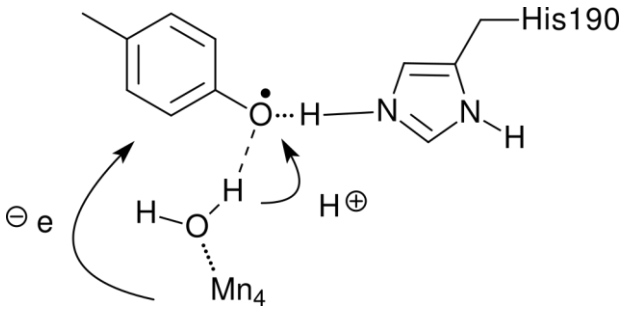

Figure 1. Example of a PCET reaction, showing the proposed mechanism for water oxidation though PCET mechanism in Photosystem II.

PCET reactions have an important ubiquity, not only in biological and organic chemistry but also in inorganic chemistry the first documented PCET mechanism involves a pH dependent reaction of the pathway between [Fe(II) - $(H_2O)_6]^{2+}$ and [Fe(III) $(H_2O)_5$ $(OH)]^{2+}$ complexes at

1952. Later, in 1981 the term of PCET was used for the first time to describe the solvent isotope effect in an electron transfer reaction between another metallic complex: $[Ru(bpy)_2(py)OH_2]^{2+}$ / $[Ru(bpy)_2(py)O]^{2+}$.[5]

Hydrogen atom transfer (HAT) reactions are described as the simultaneous transfer of an electron and a proton in the form of a hydrogen radical between the same donor and acceptor without any significant change in the charge distribution. This type of mechanism is of fundamental importance in partial oxidation and combustion processes. For example, there is evidence that dealkylation of atrazine catalyzed by cythochrome P450 follows a HAT pathway instead of a single electron transfer process (SET) in its first step (see *Figure 2).*

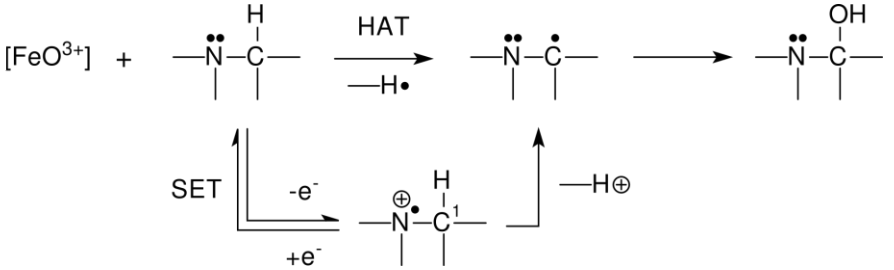

Figure 2. Example of a HAT and SET pathways. Notice that both suggested mechanisms for oxidative dealkylation are catalyzed by cytochrome P450 monooxygenase.

HAT reactions may be viewed as a subfamily of concerted PCET reactions. However, a distinction between HAT a PCET reactions is useful for the description of chemical reactions. Computational studies were performed for a better understanding of the reaction mechanisms, highlighting the difference between PCET and HAT reactions.[6-7] As a result of these computational studies, it was acknowledged that PCET reactions imply two different orbitals, one for the proton transfer and another for the electron transferred. Similarly, for HAT reactions, the proton and electron are transferred from the same starting orbital and move together in the form of a hydrogen orbital to the final orbital. *Figure 3* shows a schematic comparison among HAT, ET/PT and PCET mechanisms.

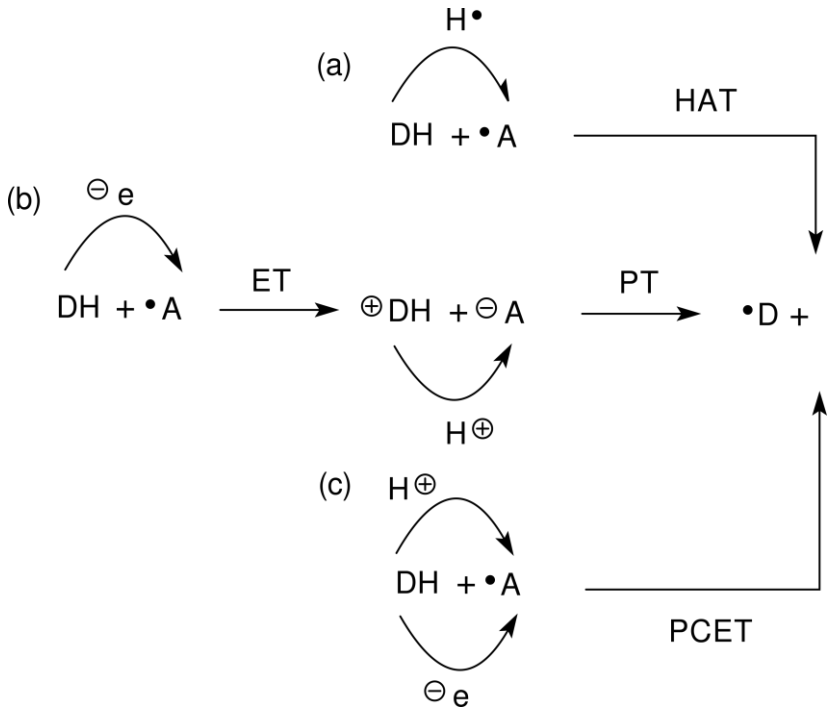

Figure 3: Schematic comparison between: (a) Hydrogen Atom Transfer (HAT), (b) Electron Transfer (ET) followed by Proton Transfer (PT), (c) Proton-Coupled Electron Transfer (PCET).

3.1.1. Orbital study

Due to the importance of the orbitals in PCET reactions and for a better understanding of the molecular orbitals that participate in the proton and electron transfer, DiLabio et al. studied the behavior and the role of lone pair-π and π-π interactions in the PCET.[8] Among other phenomena they observed that the H transfer in benzyl/toluene, a system that cannot show hydrogen bonding, can occur via PCET trough a π-stacking between HOMO and SOMO orbitals. Furthermore, they showed that the H exchange on the tert-butylperoxyl/phenol couple occurs via PCET and that the electron transfer can occur via lone pair-ring π overlap.

3.2. ANTHRANOL/ANTHROXYL PAIR

Within the PCET framework, we are interested in a recently synthesized hydrogen-bonded complex based on the anthranol/anthroxyl pair (see *Figure 4*), whose magnetic properties have been studied. It has been observed that this couple shows a different magnetic behavior at 100K and 200K: at 100K the compound shows an anti-ferromagnetic behavior, while at has undergone a magnetic phase transformation. (see *Figure 5)*.

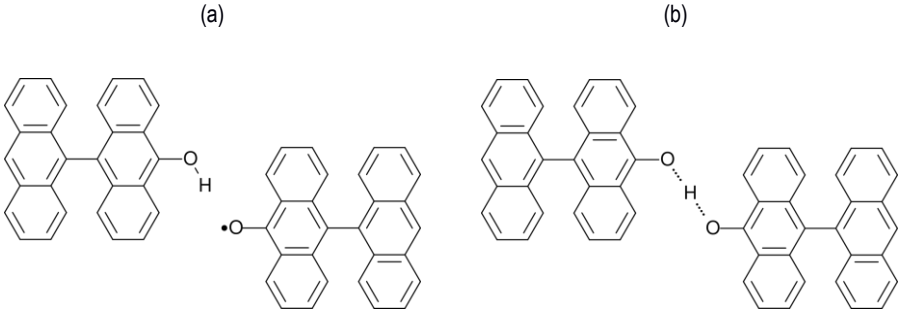

Figure 4. Anthranol/anthroxyl pair schematic structures. (a): structure at 100K, (b): structure at 200K

To explain these phenomena a model involving a proton-coupled electron transfer (PCET) process at solid state has been proposed for this pair.[1] X-ray diffraction studies of the crystalline solid showed that the proton localized at the hydroxyl group of the anthranol is inactive at 100 K (see *Figure 4a*) but reactive at 200 K, involving a reversible PCET reaction between the two molecules of the dimer where the hydrogen becomes delocalized between the dimer instead of bonded at the oxygen of the anthranol molecule, leading to a charge transfer (see *Figure 4b*).

In order to evaluate the system and check if the experimentally proposed model is valid or not several calculations and modeling of the system need to be performed.

Firstly, studies on both isolated anthranol/anthroxyl pairs at 100K and 200K will be performed in gas phase, extracting the geometry of a single pair from the crystalline X-ray diffraction data for both temperatures. The geometry of both pairs will be optimized in order to observe the changes in geometry changes that the pair undergoes without being constrained

due to the crystal packing. Besides, a transition state search will be performed with the purpose of studying the feasibility of the electron-proton transfer process.

The spin density of the anthranol/anthroxyl pairs at 100K and 200K together with the transition state will be analyzed to monitor the changes induced by the reaction. To inquire deeper into the reaction mechanism, the pairs will be modified using several functional groups to study which is the effect of electron donor and withdrawing groups from a computational point of view. Finally, the magnetic behavior of the crystal will be studied (see *Figure 5*). At 100 K, it behaves antiferromagnetically, while at 200 K it has undergone a magnetic phase transition.

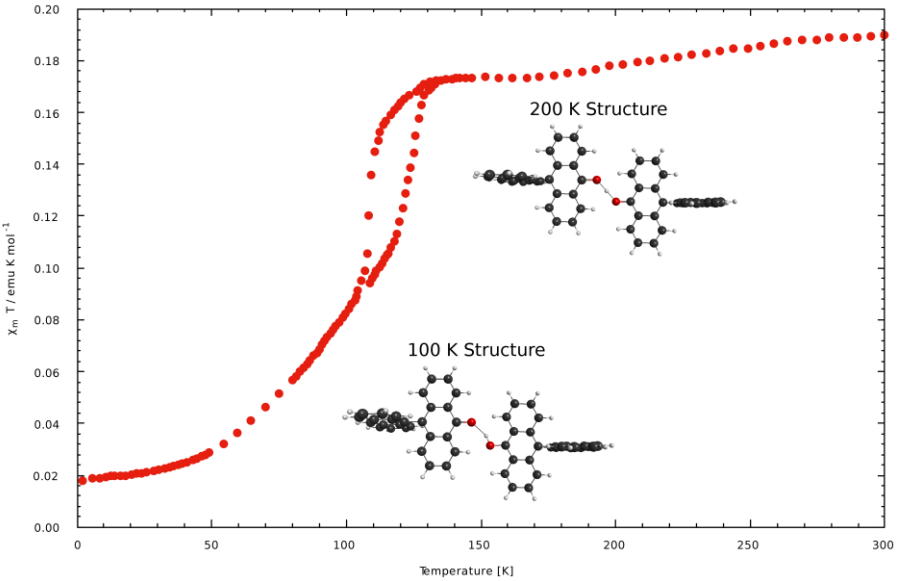

Figure 5. Magnetic susceptibility for the Anthranol/Anthroxyl crystalline solid obtained from experimental data.[1] On the left: 100 K structure of the dimer, on the right: 200 K structure of the dimer.

4. COMPUTATIONAL METHODS

4.1. METHOD AND SOFTWARE

Density functional theory (DFT) is a computational quantum mechanical modelling method used mostly in computational chemistry and physics to investigate the electronic structure in many-body systems as molecules and condensed phases. Walter Kohn was awarded with the Nobel Prize in Chemistry in 1998 for the development of the DFT. The foundations of DFT were reported in in two papers published in the 60's: Hohenberg-Kohn in 1964 and Kohn-Sham in 1965.[9-10]

The method uses a functional of the electron density to solve the Schrödinger time independent equation. DFT method is a faster option than standard *ab initio* methods such as CI, CASSCF or CC. Therefore, although *ab initio* methods can describe more accurately a molecular system, they are very demanding both regarding time and computer resources. Due to the size of the studied system, the DFT method was considered the optimal way to perform the calculations. Furthermore, literature shows that PCET reactions can be properly described using DFT theory.[3][5-8]

Due to the radical behavior of the studied system, it is necessary to use an unrestricted open shell configuration of the DFT method (UDFT) to achieve a valid description of the system.

The computational modeling program that has been used for calculations is Gaussian 09[11].

6-31+g(p,d) is a Pople basis set, which uses diffuse and polarization functions, that allows to change the topology of the orbitals used in the system. All the calculations have been performed using the UB3LYPfunctional and 6-31+g(p,d) basis set.[12-13]

Preliminary transition state search has been performed using Firefly which has been set to perform calculations at DFT/UB3LYP level and 6-31+g as basis set.[14]

4.2. TRANSITION STATE GEOMETRY SEARCH

Some problems, that include extremely slow calculation times and convergence errors in the search of the saddle point, led to the use of some strategies to find a better starting geometry for the transition state (TS) search.

Aiming to obtaining the geometry of the maximum energy between the 100K and 200K structures, a theoretical reaction pathway between them was generated. Single point energy calculations of all structures extracted from this pathway were performed in order to monitor the variation of the energy as a function of the O-H anthranol distance (See *Figure 6*).

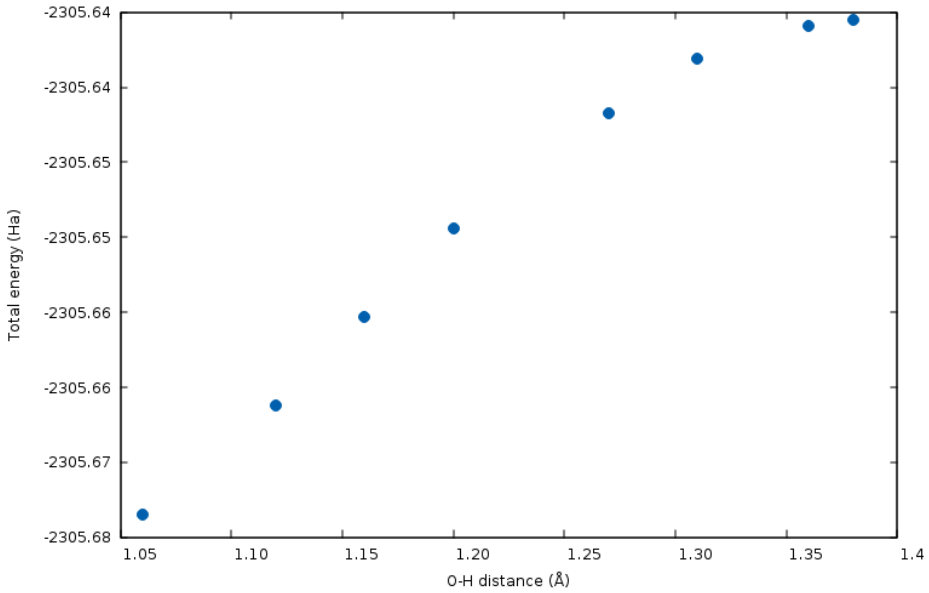

Figure 6. Energy calculations of generated pathway structures between 100 K and 200 K using an isolated dimer, extracted from X-Ray structures.

According to *Figure 6,* the last structure, with an O-H distance of 1.38 Å, corresponds to the 200 K X-Ray structure. This behavior led to consider the 200 K structure as a semi transition state. As a result, the 200 K X-Ray has been used adequately as the starting geometry for saddle point calculations. The TS point geometry was finally obtained using a 6-31+G basis set with Firefly software (as mentioned in the previous section 4.1).

4.3. MODEL STRUCTURE

In order to speed up some heavy and problematic calculations, a model structure of both anthranol/anthroxyl pairs at 100 K and 200 K has been build and tested. This structure consists in an anthranol/anthroxyl pairs in which the back anthracene ring attached to the carbon at position 9 (see *Figure 7a* for anthracene ring numeration) is replaced with a methyl group, which decrease the size of the molecule (see *Figure 7*).

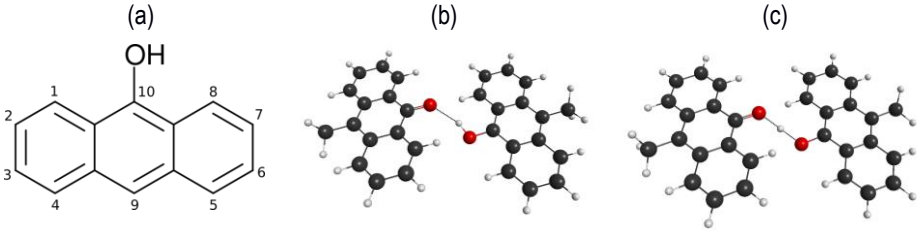

Figure 7. Anthranol numeration (a). Model structure for the 100 K dimer (b) and for the 200 K dimer (c) X-Ray structures.

4.4. MAGNETIC SUSCEPTIBILITY CALCULATION METHOD

The magnetic susceptibility of the anthranol/anthroxyl crystal will be calculated using a first-principles bottom-up procedure (FPBU). An analysis of the crystal packing will be performed to select pairs of radicals to compute all the possible J_{AB} magnetic interactions between A-B radicals. The value of the J_{AB} magnetic coupling of each pair will be calculated as the energy difference between the open shell singlet and triplet states of each pair using DFT. With calculated J_{AB} values the magnetic topology and a magnetic model for each phase will be proposed. A full diagonalization of each magnetic model will be performed in order to compute the energy spectra and spin quantum numbers. Finally, using the statistical mechanics expression of $\chi T(T)$, the magnetic susceptibility will be calculated for each model in a defined range of temperatures and compared to the experimental data.

5. OBJECTIVES

The main purpose of this study is the evaluation of the thermodynamics and the magnetic behavior of the recently synthesized anthranol/anthroxyl solid at two different temperatures upon phase transition.

To evaluate the thermodynamical behavior of the anthranol/anthroxyl pair, the study of an isolated dimer using computational methods will be performed. The main goal of the calculation will be to explore in detail topological changes of the solid involved in the PCET reaction.

Furthermore, the effect of the electron withdrawing and donating groups will be considered in order to propose alternatives to the anthranol/anthroxyl solid that might favor the PCET reaction.

The study of the magnetic behavior at 100 K and 200K aims at identifying and evaluating the anthranol/anthroxyl radical pairs that are magnetically coupled.

Finally, our objective will be to determine the corresponding magnetic topology and calculate the resulting magnetic susceptibility data, which will be compared to experimental data.

6. RESULTS AND DISCUSSION

6.1. THERMODYNAMICAL EVALUATION OF THE ISOLATED ANTHRANOL/ANTHROXYL DIMER SYSTEM

To evaluate the energy profile the anthranol/anthroxyl system, single point energy calculations were performed using the optimized geometry of the anthranol/anthroxyl pair at 100 K and 200 K. Isolated dimers have been selected and extracted from the X-ray structure cited at [1] and are shown in *Figure 8*.

As can be seen in *Figure 8*, the 100 K (A-B-C) structures consist in an anthranol molecule next to an anthroxyl radical, while in the 200K (E-F) structures the dimer consists in two semi-radicals with a hydrogen atom shared by both oxygens. Due to the limitations of the X-ray diffraction technique, hydrogen atoms cannot be detected. The position of the hydrogen atoms of both structures was manually introduced and refined through optimizations. All calculations were performed at gas phase and are temperature independent.

Full optimization of X-Ray 100 K (C) structure leads to structure A, with an energy difference of 5.96 kcal·mol^{-1}, while a constrained optimization (distances between the O-O and the O-H are frozen during the optimization), leads to structure B, with an energy difference of 1.30 kcal·mol^{-1} from A structure. In comparison with the X-Ray 100 K (C) structure, the anthracene groups in both A and B structures rotate but in a different way in each optimization. While in the A structure, which has it is less sterically hindered than B, the anthracene groups rotate to align the hydrogen atom with both oxygens, the B structure with frozen coordinates performs a larger rotation in order to stabilize the dimer.

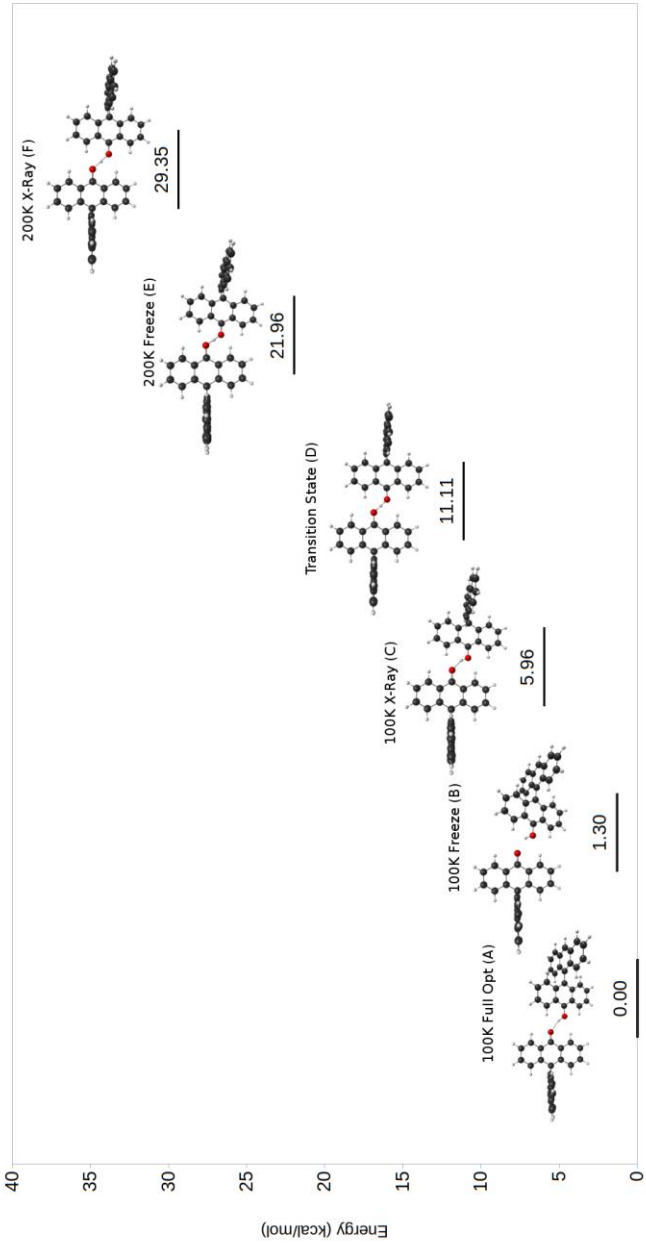

Figure 8. Energy profile of the PCET reaction in terms of an isolated anthranol/anthroxyl pair. Note the energy of A has been taken as a reference.

Full optimization calculations of X-Ray 200 K (F) structure leads to the A structure. This can be interpreted considering that the F structure is not a local minimum but a maximum in the reaction pathway. According to *Figure 6*, F could be a maximum in the potential energy surface. The symmetry of the A structure yields to two similar but enantiomeric structures acting both as a reactant as well that as a product (see *Figure 9*). The F structure can be regarded as a structure that might be close to the transition state. When a full optimization is performed on this structure, depending on the algorithm and the accuracy of the coordinates, one or another enantiomer will be obtained (see *Figure 9*).

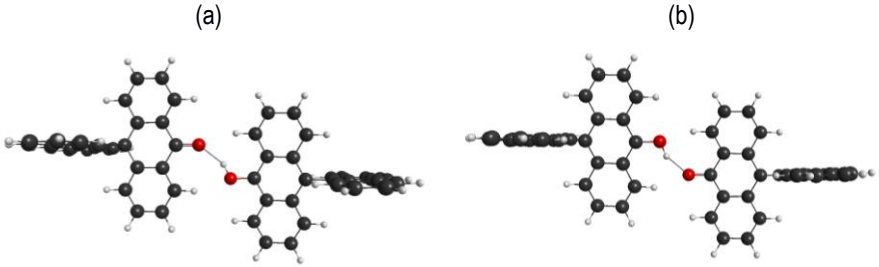

Figure 9. The two possible enantiomeric conformations of A structure.

A constrained optimization of F (keeping constant the O-H-O distance) is required to obtained the E minimum. Minor rotation of both anthracene ring is present in this structure, note that the rotation is much less abrupt (dihedral C8-C1-C8'-C1' = 5.4°) that the one observed in both A and B structures compared to C structure (dihedral C1-C8-C1'-C8' = 26.9°, 28.3º and 5.2º respectively). However, the energy stabilization between F and E is higher (7.39 kcal·mol^{-1}) than the energy difference between C and A (5.96 kcal·mol^{-1}).

The rotation of the back 9-anthracene observed in both structures (see *Figure 7* for numbering), along with the alignment of the O-O atoms when an optimization calculation is performed, indicates that in the crystal the back 9-anthracene has a structural role, and restricts the mobility in the reaction pathway. This mobility restriction may help the PCET reaction to occur avoiding several rotations after or during the PCET reaction.

6.1.1. TRANSITION STATE

The transition state structure is the cornerstone of the PCET reaction in order to describe the reaction pathway and mechanism.

The transition state (D) resembles the 200 K structure (F) (see *Figure 10*). Overlap of D and F shows that the geometry difference between both is minimal. But for the distance between the Oxygen atoms, which changes drastically from 7.76 in F to 2.41 in D. This fact will be discussed deeply in the next section.

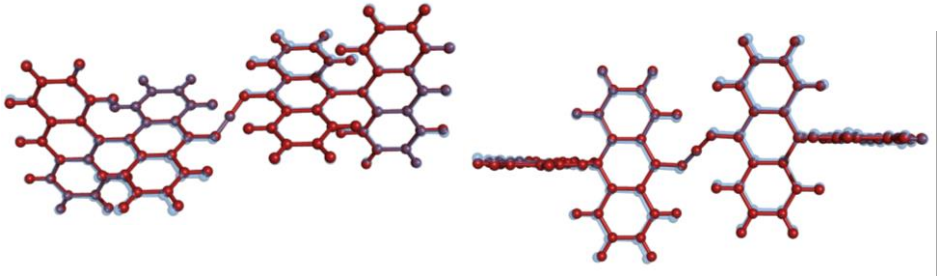

Figure 10. D structure (TS, red) and F structure (X-Ray 200 K, blue) overlapped together from two different views.

Structure D has been characterized as TS after a vibrational analysis. The imaginary frequency of D (see *Figure 11*) shows a single vector placed in the H atom and pointing to one of the both oxygen atoms, validating that the hydrogen atom has the most important role in the PCET reaction.

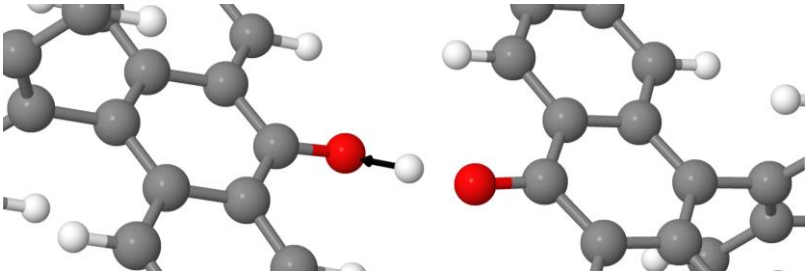

Figure 11. Imaginary frequency vector representation (black) of 200 K X-Ray structure.

Unlike optimized A, B and E, structures, D has the two back 9-anthracene rings oriented parallel to each other. If the PCET reaction starts from A, both back 9-anthracenes need to be oriented in the correct form in order for the reaction to occur. As commented previously, the mobility restriction that comes with the crystalline packing apparently reduces the activation energy of the reaction. While the activation energy between the full optimized 100 K structure

(A) and the transition state structure (D) is 11.11 kcal mol^{-1}, the activation energy if starting from X-ray structure (C) is 5.15 kcal mol^{-1}. Not only the back 9-anthracene positions of D and F agree with each other but also the O-O and O-H distances seems to match between both structures.

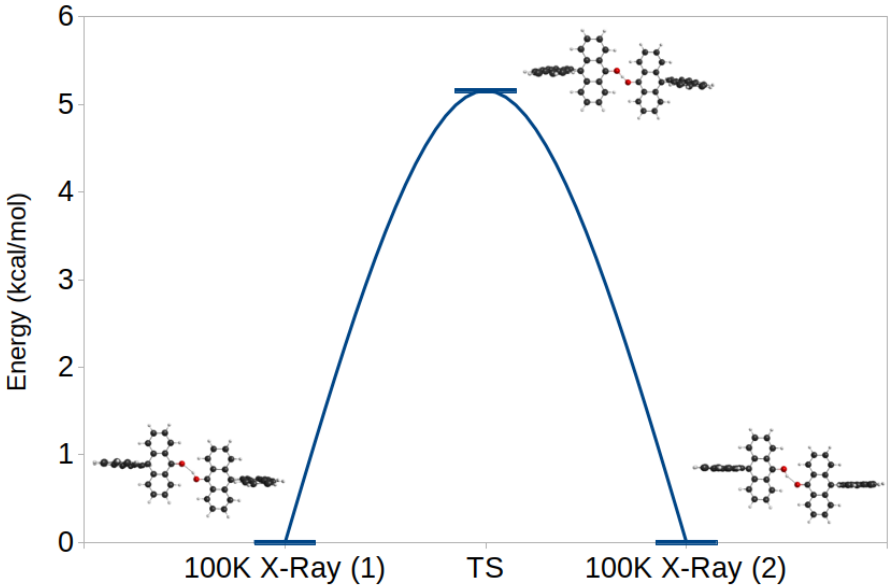

Figure 12. Symmetric reaction pathway of the PCET reaction between both enantiomers.

The symmetry of X-Ray 100 K (C) structure leads to two enantiomeric structures with the same activation energy (see *Figure 12*), This fact, together with the lesser activation energy if packing is taken into account, yields to a repetitive forward and backward PCET reaction between the two enantiomeric structures when the solid reach the necessary temperature to surpass the activation energy. Along with the uncertainty in the position of the transferred hydrogen and the resemblance of the D and F structures, this behavior leads to think that the crystal structure studied at 200 K could be a statistical average of all the structures included in the pathway of the PCET reaction, in which the hydrogen between the two oxygens is delocalized and constantly moving between both oxygens.

Further studies implying molecular dynamics are required in order to study the statistical behavior of the solid at 200 K, as already done in DTA- based compounds.[15] However, due to time limitations, this TFG project could not address that issue.

6.1.2. BOND DISTANCES ANALYSIS

Bond distances between the atoms involved in the PCET reaction (see *Table 1)* are the key point in order to understand the reaction between the anthroxyl/anthranol pair.

Structure	Key	O-O [Å]	O-H (Radical) [Å]	O-H (Hydroxyl) [Å]
100K Full Opt	A	2.78	1.85	0.98
100K Freeze Opt	B	2.77	1.97	0.84
100K X-Ray	C	2.77	1.97	0.84
Transition State	D	2.41	1.20	-
200K Freeze	E	2.76	1.38	-
200K X-Ray	F	2.76	1.38	-

Table 1. O-O distances and O-H shortest distances for A to F structures. Distances in Å.

The O-O distance varies slightly between X-Ray and optimized minimum structures but varies significantly in the transition point (D) structure. The approach of both monomers at the transition point (O-O distance is 2.41 Å) facilitates the hydrogen and electron transfer between the two monomers. Comparing the two X-Ray C and F, the O-O distance in both structures varies slightly being smaller in F.

As mentioned previously, the 200 K X-Ray structure is not a real minimum in the potential energy surface. We have thought about two possible explanations for this phenomenon. It could be possible that the distance between both oxygens necessarily decreases in the crystal structure while the PCET reaction is proceeding. However, if the hydrogen atom remains more time near the oxygens than in the center of the dimer, it is possible to observe no change or a slightly change in the O-O distances depending on the statistical distribution. Another possibility is that the restricted mobility of the dimers in the crystal packing precludes the movement of both monomers, increasing the activation energy and going through another transition state with a larger O-O distance. Both options could explain the big difference between D and F. Nevertheless, for a more accurate description of the structures included in the PCET reaction pathway a molecular dynamic study would need to be performed in order to find the statistical distribution of all the possible conformations that the anthroxyl and anthranol can adopt within the dimer due to thermal fluctuations.

Notice that longer O-H distance between O in anthroxyl radical and H atom and shorter O-H distance in the hydroxyl group is observed in C compared to the optimized structure. This can be translated into a larger tendency of full optimized A structure to undergo the PCET reaction. However, energetics indicates the contrary (see *Figure* 8). Therefore, it might be possible that the hydrogen atom is not correctly placed in the X-Ray structure due to the bad characterization of hydrogen atoms that is implicit in X-Ray diffraction characterization technique.

6.1.3. MOLECULAR ORBITALS ANALYSIS.

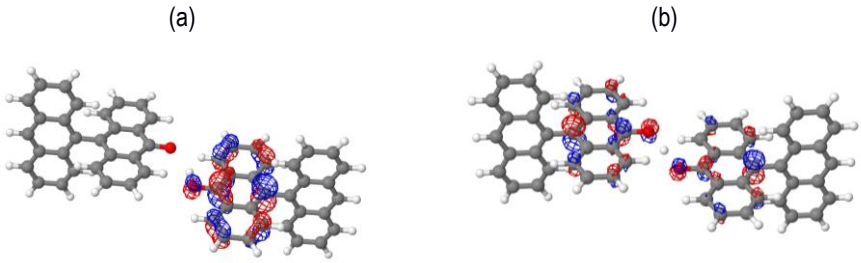

Figure 13. (a) HOMO of the 100K X-Ray structure (C). (b) HOMO of the 200K X-Ray structure (F)

Figure 13 shows the representation of the Highest Occupied Molecular Orbital (HOMO) for both 100 K and 200 K X-Ray structures. At 100 K, the HOMO of C is distributed only over the anthranol molecule, while at 200 K the HOMO of F splits equally into the two semi-radicals. For F, a bonding behavior between the lone π-orbitals of both anthranol/anthroxyl oxygens can be observed (see *Figure 13b*). Literature shows that in some transoid PCET reactions involving aromatic compounds, non-bonding orbitals could transform into partially bonding orbitals when the PCET reaction reach the transition state structure.[8]

6.2. MAGNETIC PROPERTIES EVALUATION OF THE ANTHRANOL/ANTHROXYL CRYSTAL

Anthroxyl/anthranol crystal shows AFM properties while it remains at low temperature (<100 K). However, when the crystal reaches a temperature of 130 K the crystal undergoes a magnetic phase transition. At 200 K, an experimental χT value of 0.19 emu K mol^{-1} is finally reached. Therefore, for studying magnetism purposes, the anthroxyl/anthranol geometries used in this section refer always to X-Ray 100 K and 200 K crystal structures

Phase transition from a P-1 with *a* = 11.820(2) Å, *b* = 13.800(3) Å, *c* = 14.548(3) Å, α = 95.716(4)°, β = 92.642(3)° and γ = 111.648(3)° at 100 K to P-1 with *a* = 9.175(3) Å, *b* = 9.637(3) Å, *c* = 13.870(6) Å, α = 98.729(7)°, β = 108.343(6)° and γ = 101.986(9)° at 200 K has been proposed to explain the change of the magnetic behavior of the system. As seen in the thermodynamical explanation, the 200 K structure of the crystal consists only in one semi-radical (anthroxyl) that repeats into the solid (see *Figure 7c*). Contrarily the 100 K structure consists in a dimer composed by one radical (anthroxyl) and an anthranol molecule in a face-to-face O (anthroxyl)···HO (anthranol) arrangement (see *Figure7b*).

Due to computational difficulties and to decrease the calculation times, all the calculations have been performed using the model structure proposed in section 4.2, where the back 9-anthracene has been replaced by a methyl group.

6.2.1. SPIN DENSITY ANALYSIS

Due to the radical and semi-radical nature of both structures at 100 K and 200K, respectively, spin density studies have been made through single point calculations using the X-Ray structures C and F (see *Figure 14).*

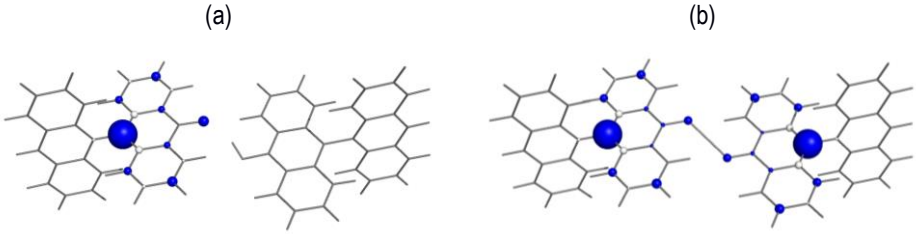

Figure 14. Spin density scheme of the (a) X-Ray 200 K F and (b) X-Ray 100 K C structures. Blue color represents positive spin density while white color represents negative spin density.

For the 100 K X-Ray structure, the spin density is only distributed over the anthroxyl radical molecule. For the 200K X-Ray (F) structure, the spin density is evenly delocalized on both anthroxyl semi-radical molecules. For both structures, the spin density is mostly concentrated over the carbon at 9 position attached to the anthracene main ring. Note that the back 9-anthracene ring presents no significant spin density, except for the carbon atom directly

attached to the carbon at position 9 that presents a slightly negative spin density, since it orientates perpendicular to the main anthracene ring.

The distribution of the spin density in the main anthracene can be explained through the aromaticity of the anthracene molecule (see *Figure 15*). The spin density is distributed starting from the oxygen atom of the radical at 100 K, or semi-radical in the 200 K structure, in two directions of the anthracene ring, corresponding to carbons at 8 and 1 positions. The anthracene ring loses its aromaticity in the carbon number 9, that receives the spin density from both directions, resulting in a larger spin density accumulation. Moreover, this loss of aromaticity prevents the back 9-anthracene to receive spin density from the main anthracene ring.

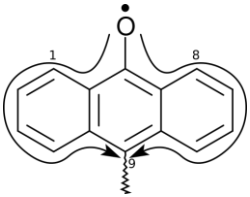

Figure 15. Scheme of the aromaticity distribution of the spin density in the main anthracene.

Annex 1 shows the total spin density of some atoms in both X-Ray 200 K and X-Ray 100 K structures. Comparison between absolute spin density of each atom of the anthroxyl molecule in the X-Ray 100 K dimer and to the absolute density of the corresponding atoms in both semi-radicals of the X-Ray 200 K structure, shows an equivalent distribution of the spin density on both semi-radicals. The absolute distribution of the spin density in each semi-radical at 200 K is half of the absolute spin density distribution in the anthroxyl radical at 100 K.

The spin density transfer can be seen as a progressive transfer that comes from the anthroxyl radical and goes to the anthranol molecule until the last becomes the radical anthroxyl and obtains the spin density of the first anthroxyl.

The transition state (D) shows a spin distribution similar to that shown by the X-Ray 200 K structure (see *Figure 16*). Due to the similarities between the TS and X-Ray 200 K structures depicted in section 6.1, the spin density in each one of the two semi-radicals in the 200 K crystal, seems to oscillate depending on the position of each radical pair in the pathway of the PCET reaction. This leads to a potential magnetization of all single molecules packed in the solid structure. This behavior is very different at 100K, where only half of the molecules packed in the crystal carries larger spin density than that observed on each semi-radical at 200 K.

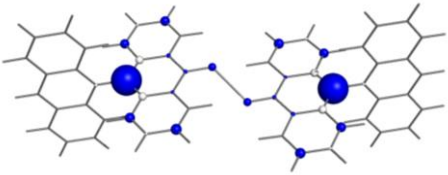

Figure 16. Spin density scheme of the D structures. Blue color represents positive spin density while white color represents negative spin density.

To determine the viability of the model structures for the J_{AB} calculations, the spin density distribution has been calculated for the 100 K, 200 K and TS model structure in order to compare it with the values obtained for the complete structure (see *Figure 17*).

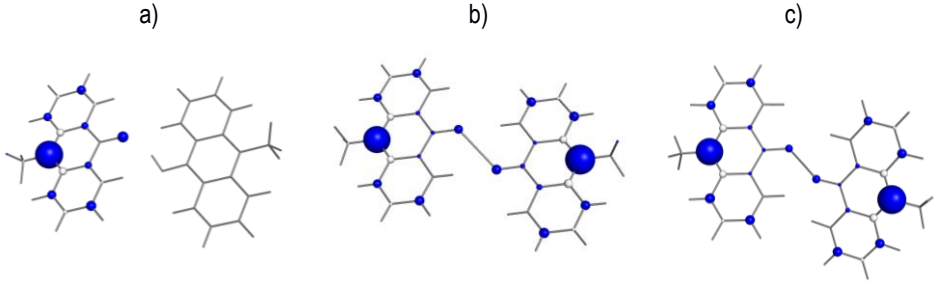

Figure 17. Spin density scheme of the model (a) 100 K, (b) 200 K and (c) transition state model structures. Blue color represents positive spin density while white color represents negative spin density.

The spin density in the model structures is distributed in a similar way that in the complete structure.

6.2.2. MAGNETIC MODEL EVALUATION, STUDY OF J_{AB} MAGNETIC COUPLINGS

Several pairs of dimers have been extracted from the crystal structure of the solid at both 100 K and 200 K. To check the magnetic interactions between all the pairs, calculations of open shell singlet and triplet states have been performed using all pairs extracted from the crystal structure. Pairs with a distance longer than 14 Å have been excluded.

The back 9-anthracenes have been replaced by a methyl in all the pairs in order to decrease the calculation time.

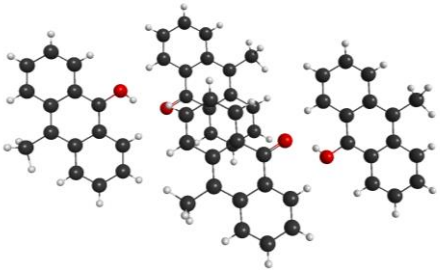

O-O Radical distance 7.13 Å (100K7)

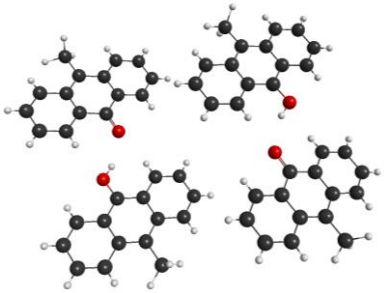

O-O Radical distance 8.63 Å (100K8)

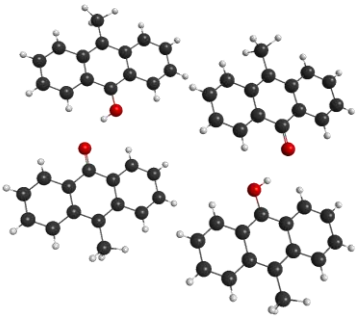

O-O Radical distance 11.22 Å (100K112)

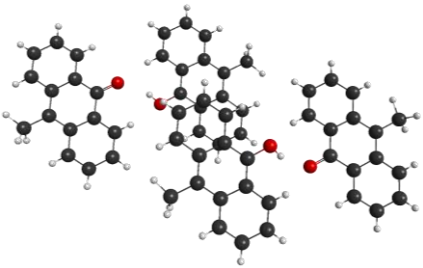

O-O Radical distance 11.56 Å (100K115)

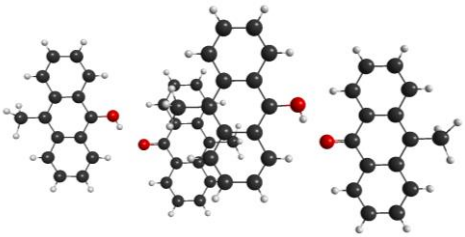

O-O Radical distance 11.82 Å (100K118)

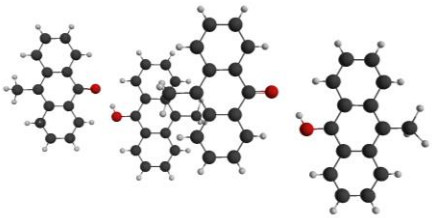

O-O Radical distance 13.80 Å (100K13)

Figure 18. Pairs of anthroxyl/anthranol radicals selected to evaluate the J_{AB} magnetic coupling at 100 K

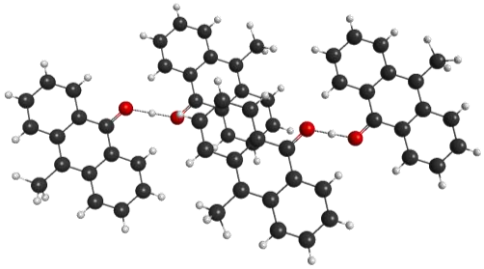

semi-radical distance 7.24 Å (200K7)

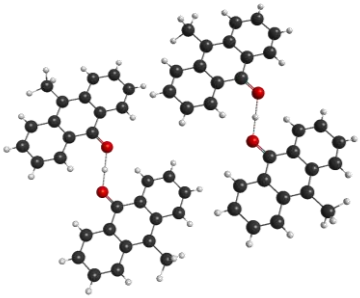

semi-radical distance 8.82 Å (200K8)

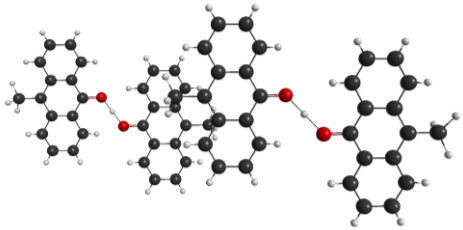

semi-radical distance 11.85 Å (200K11)

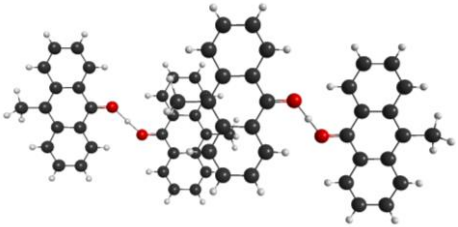

Radical distance 13.87 Å (200K13)

Figure 19. Pairs of anthroxyl/anthranol radicals selected to evaluate the J_{AB} magnetic coupling at 200 K

Figures 18 and 19 show the different pairs extracted from the crystal structure at 100K and 200K, respectively. Note that 100K7 and 100K115 are equivalent to 200K7, 100K8 and 100K112 are equivalent to 200K8, 100K118 is equivalent to 200K11 and 100K13 is equivalent to 200K13. The structures gain symmetry in the transition from 100 K to 200 K. This fact removes the presence of some 100 K pairs because the hydrogen atom is equally shared by the anthroxyl semi-radicals.

Triplet and open shell singlet energy calculations were performed in order to evaluate the J_{AB} coupling interactions of all pairs. Only 100K7 and 200K7 presented a magnetic coupling interaction different from zero. The magnetic coupling has been calculated to be -96.92 cm^{-1} for 100K7 structure and -63.22 cm^{-1} for 200K7. Calculation of J_{AB} for the 200K7 pair has required a

model that explicitly takes into account the 2 semi-radicals at O-O 7.24 Å distance, while the other 2 semi-radicals are replaced by their corresponding Merz-Singh-Kollman point charges (see *Figure 20* a).[16] This model has been validated against J_{AB} calculation for 100K7 pair. For the 100K7 pair J_{AB} has been evaluated using both a full-radical and a radical-charges model with a value of J_{AB} of -106.60 cm^{-1} and -101.22 cm^{-1}, receptively (see *Figure 20* b and c).

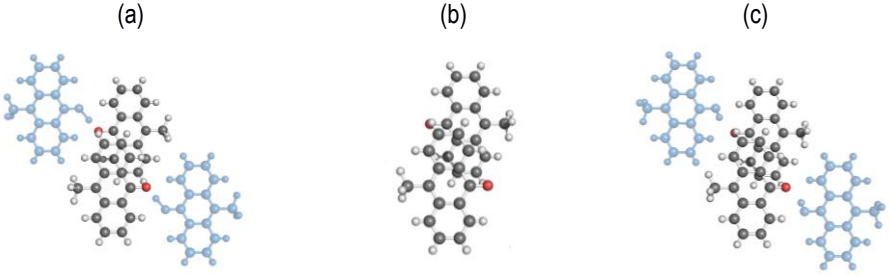

Figure 20. a) 200K7 structure with Merz-Singh-Kollman point charges (transparent blue), b) 100K7 full-radical structure, c) 100K7 radical-charges (transparent blue) structure.

The analysis of the geometry of 100K7 and 200K7 indicates that the J_{AB} magnetic coupling is due to the partial overlap between the anthracene rings of two different anthroxyl radicals. Note that 100K115 also shows partial overlap between anthranol molecules instead of anthroxyl radical. However, 100K115 shows no magnetic coupling because anthranol has no net spin density.

Distances between the two overlapped anthracene rings vary 0.1 Å between the 100K7 (3.7 Å) and the 200K7 (3.8 Å) structures (see *Figure 21*). It is known that the value of the J_{AB} magnetic interaction depends on the inter planar radical-radical distance.[1] Therefore, the difference between J_{AB}'s at 100K7 and 200K7 is due to major coupling at shortest distances.

Figure 21. Local view of the anthracene overlapping, showing C-C distances in Å. At the left the 100K7 structure, at the right the 200K7 structure.

6.2.3. CALCULATION OF MAGNETIC SUSCEPTIBILITY

The magnetic topology at 100 K is driven by the AFM J_{AB}^{100K7} magnetic interaction (-96.92 cm^{-1}). It consists of isolated 0D AFM dimers (see *Figure 22a*). At 200 K, the magnetic topology is defined in terms of J_{AB}^{200K7} = -63.22 cm^{-1}. It consists in 1D isolated spin chains (see *Figure 22b*). The change of the magnetic topology is due to the transformation of the anthranol into an anthroxyl semi-radical at 200 K. At 100 K only the anthroxyl radicals, representing the 50% of the total number of molecules of the crystal, present magnetic coupling. Contrarily at 200 K all the molecules of the solid have a semi-radical behavior. Therefore, all molecules are equivalent and the isolated 0D dimers at 100 K becomes a 1D chain at 200 K.

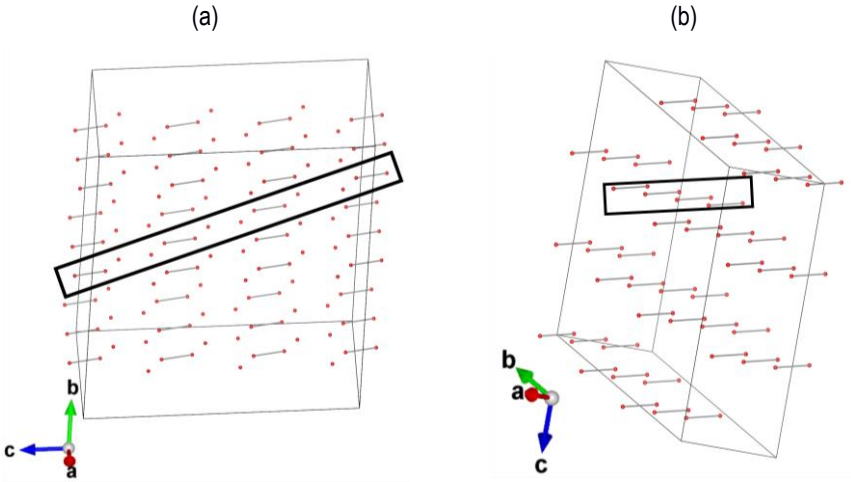

Figure 22. Magnetic topology of the anthranol/anthroxyl crystal where each molecule is replaced by its oxygen atoms. (a) At 100 K, it consists of isolated AFM pairs of radicals. (b) At 200 K, it consists of isolated 1D AFM chains. The representation only shows the connection between the oxygen of the molecules that have magnetic coupling. Note that the large cubes are only for aesthetic purposes and do not represent the unit cell.

A subset of the magnetic topology of both crystal structures has been studied through a proposed magnetic model consisting in 10 radicals for both 100 K and 200 K (see *Figure 22 (a) and (b)* respectively) structure. A full diagonalization has then been performed for the 100 K and 200 K models in order to obtain the energy spectrum and corresponding spin values of each model. Using this energy spectrum and the statistical mechanics expression of $\chi T(T)$, the

magnetic susceptibility has been calculated for a range of temperatures ranging from 0 K to 300 K, using a gyromagnetic g constant with a value of 2.0033, and a magnetic field with a value of 1 T, in order to compare the calculations with the experimental results.[1] (see *Figure 23*).

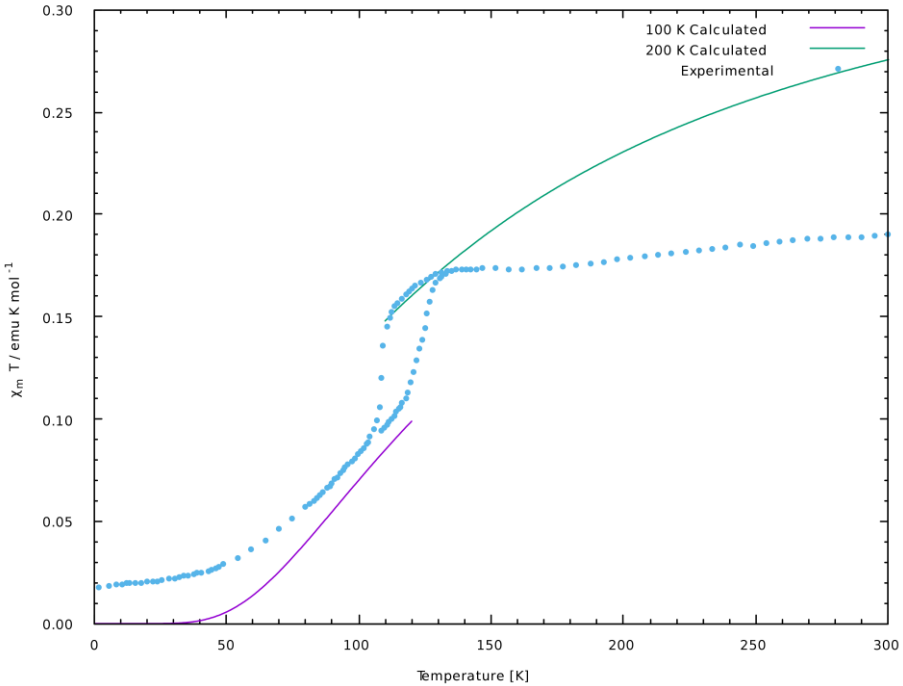

Figure 23. Molar magnetic susceptibility (emu K mol^{-1}) in front of temperature (K). Experimental (dot blue), 100K calculated (line purple), 200K calculated (line green).

Figure 23 shows the representation of magnetic susceptibility in front of temperature for experimental, 100 K calculated and 200 K calculated states. Experimental behavior of the crystal is between both calculated values of magnetic susceptibility.

The calculated magnetic susceptibility at 0 K is negligible compared with the experimental values. Impurities contained in the crystal or an unknown phase can be the origin of the magnetic susceptibility difference at this temperature. Starting from 50 K, the experimental and our calculated χT values using the 100 K data, increases following the same rate until the temperature reaches a value of 100 K. There is a sharp increase in the χT region ranging from

100 K and 135 K. This is probably due to the aspect that dimers have the necessary energy to start the PCET reaction. When the necessary amount of energy to activate almost every dimer of the solid is reached, in the region of 135K, the prevalent structure found in the solid can be the X-Ray 200 K structure (F) and the pairs behave in the same way that *Figure 22b* model. Contrary, the similar behavior of the 100 K theoretical calculations and experimental magnetic susceptibility in the section between 50 K and 100 K, indicates that the crystal behaves like the model proposed for the 100 K showed in *Figure 22a*, pointing that the prevalent structure in this segment is the 100 K X-Ray structure (C).

At 300 K, the experimental χT value is *ca.* 0.19 emu K mol^{-1}. This is not the value expected for χT for a S = ½ at high temperatures. The value of a solid composed solely by S = ½ anthroxyl radicals has a χT value of 0.375 emu K mol^{-1} at high temperatures. In the literature, it is said that the experimental value of 0.19 emu K mol^{-1} at high temperatures corresponds with to the value of only the 50% ($0.375/2 \approx 0.19$ emu K mol^{-1}) of the molecules of the solid behaving as a S = ½ radical.[1] Nevertheless, our studies show that at high temperatures all the molecules of the system behave as a semi-radical.

In addition, the calculated χT gap between 100 K and 200 K agrees with the experimental magnetic phase transition χT gap.

6.3. EFFECT OF THE SUBSTITUENTS

To study the behavior of the PCET reaction into different scenarios, different functional groups have been used to replace the back 9-anthracene of the anthranol/anthroxyl (X-Ray 100 K structure, C).

As seen in previous sections, the major accumulation of spin density is located over the carbon number nine in both molecules, this led us to think that a substitution of the back 9-anthracene ring could change significantly the behavior of the reaction. Therefore, the back 9-anthracene ring of the original anthranol/anthroxyl pair was replaced by five functional groups with different electron withdrawing or electron donor character. The five functional groups selected are (from more to less electron withdrawing character): -CN, -F, -Br, -SH and $-CH_3$. The groups were chosen with the aim of presenting different values within the scale of the inductive effect.

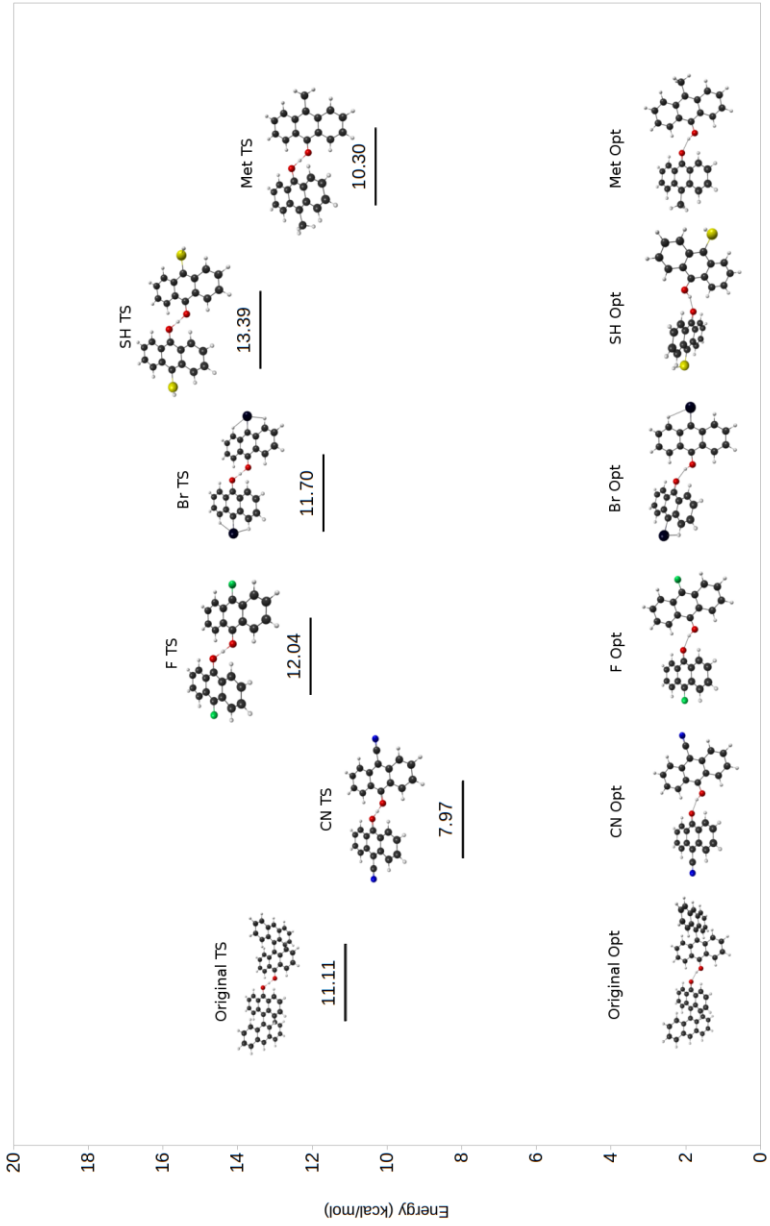

Figure 24. Energy profile of the PCET reaction for each substituted anthranol/anthroxyl pair. Note the energy of full optimized structure of each pair has been taken as a reference.

Optimization calculations has been performed for each new pair with the new functional groups. The transition state structure together with the full optimized structure are the two key structures to determine the activation energy of the reaction. Several transition state searches have therefore been done for each new pair, starting from a substituted TS structure (D).

To properly study the inductive effect, a global study of the activation energies has been performed. In addition, an individual study of the geometry of both optimized and TS structures, compared with the original structures has been conducted.

6.3.1. ACTIVATION ENERGY ANALYSIS

Figure 24 shows the relative activation energy of each dimer with respect to the energy of its full optimization structure. The groups have been ordered from more to less electron withdrawing character.

The activation energy of the different groups does not seem to follow any pattern related with the inductive effect. CN and Met substituted structures have a smaller activation energies (7.97 kcal mol^{-1} and 10.30 kcal mol^{-1}, respectively) than the original structure, while the F, Br, and SH substituted structures require higher activation energies (12.04 kcal mol^{-1}, 11.70 kcal mol^{-1} and 13.39 kcal mol^{-1}, respectively) than the original structure.

Halogen structures present a similar activation energy, but the required energy is slightly smaller in the Br structure. Since Br is slightly less electron withdrawing than the F atom, this could be the cause of this effect. Further calculations in order to study the different behavior of the halogens are needed, but are out of the range of this work.

Both CN and SH substituted structures present an unexpected behavior. While in the F and Br substituted structures, which have strong electron withdrawing groups, the activation energy increases, the CN group substituted structure, with a strongest electron withdrawing character, decreases significantly the activation energy. The same behavior but reversed seems to occur with the SH substituted structure. Methyl is a strong electron donor group, and when replaces the back 9-anthranol of the original structure, decreases the activation energy. A similar effect is expected for the SH substituted structure, which also is considered an electron donor, but contrary to expected, it is the group which increases more the activation energy.

6.3.2. BOND DISTANCES ANALYSIS

Table 2 shows the bond distances between the atoms involved in the PCET reaction of the anthranol/anthroxyl pair and the substituted structures. Note that these bond distances vary slightly from the optimized and TS original structures. The distances needed for the PCET reaction to occur seem to be constrained and only a few deviations are allowed. However, the substituted 9-carbon is far away from the atoms that are involved in the PCET reaction. Further calculations could be made replacing the hydrogens attached to the carbons number 2 and 7 to study whether the bond distance is more roughly distorted.

Structure	O-O [Å]	O-H (Radical) [Å]	O-H (Hydroxyl)[Å]
100 K Full Opt	2.78	1.85	0.98
Transition State	2.41	1.20	-
CN Full Opt	2.77	1.83	0.98
CN-TS	2.39	1.19	-
F Full Opt	2.78	1.84	0.98
F TS	2.41	1.20	-
Br Full Opt	2.77	1.83	0.98
Br TS	2.41	1.20	-
SH Full Opt	2.77	1.84	0.98
SH TS	2.41	1.20	-
Met Full Opt	2.78	1.85	0.98
Met TS	2.40	1.21	-

Table 2. O-O distances and O-H shortest distances for all the substituted structures.

6.3.3. GEOMETRY AND SPIN DENSITY DISTRIBUTION

Compared with the original anthranol/anthroxyl structure, the optimized CN-structure only varies in the angle between the two anthranol and anthroxyl (dihedral C8-C1-C8'-C1' = 37.9º) and without major deviations with respect the other substituted structures (see *Figure 25*). The two key points of CN-structure are the spin density and the deviation from the original TS structure (dihedral C8-C1-C8'-C1' = 16.9º). While the other substituted structures, except the substituted Methyl-TS structure, change slightly from the original TS structure, the presence of the CN-group in the carbon 9 yields to a transition state with the two molecules of the pair in the same plane. Moreover, the spin density distribution in this structure delocalizes over the C and N atoms, removing some spin density from the 9 carbon.

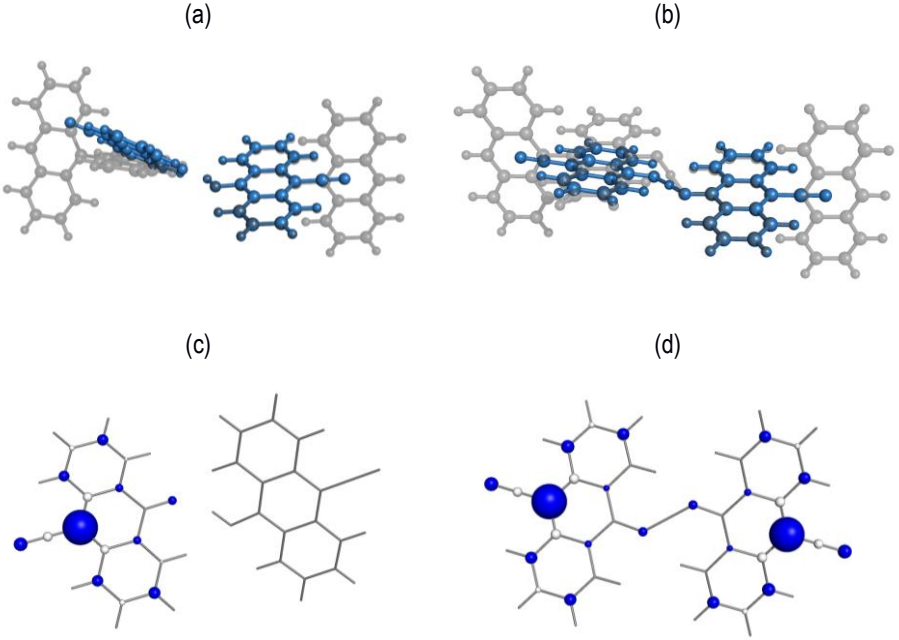

Figure 25. Overlap between (a) CN-substituted and C original anthranol/anthroxyl minima, and (b) CN-substituted D original anthranol/anthranol TS structures. Spin density distribution of CN-substituted (c) minimum and (d) TS.

Compared with the original anthranol/anthroxyl full optimized structure, the F-substituted structure angle varies slightly (dihedral C8-C1-C8'-C1 = 37.1º) between the anthranol and anthroxyl molecule (see *Figure 26*), like the other substituted structures. However, the transition state of F-structure, highly resembles the TS original structure. The density distribution of both TS and optimized F-structure, also resembles its respective original structures, with no spin density over the F-atom.

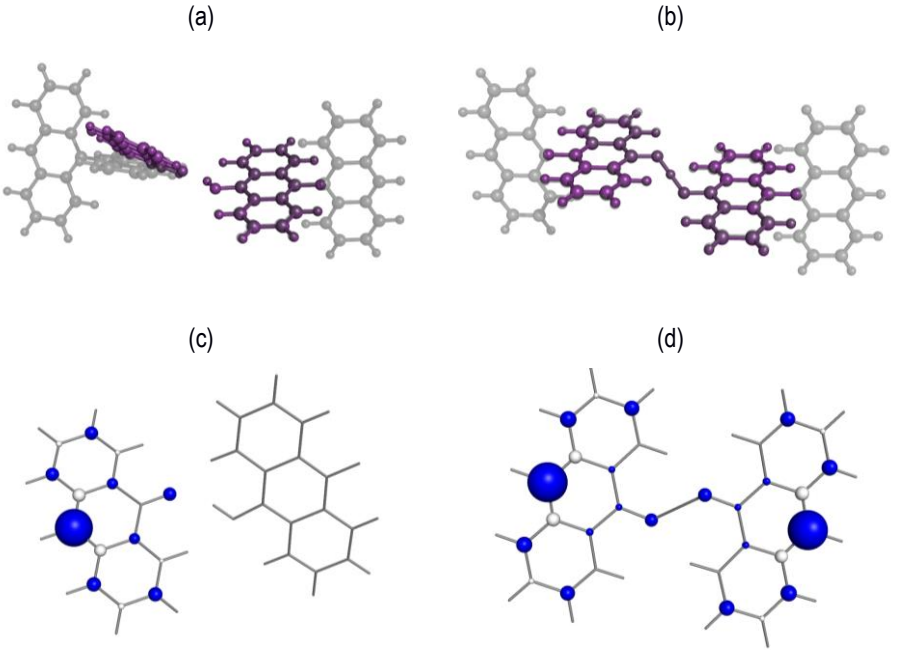

Figure 26. Overlap between (a) F-substituted and C original anthranol/anthroxyl minima, and (b) F-substituted D original anthranol/anthranol TS structures. Spin density distribution of F-substituted (c) minimum and (d) TS.

Br-substituted structures behave similar to F-substituted structures (see *Figure 27*). The angle between the anthranol/anthroxyl pair is slightly bigger (dihedral C8-C1-C8'-C1' = 39.4º) than in the F-structure. Like the F-TS structure, the Br-TS structure resembles the original TS structure. In terms of spin density, the Br-derivatives structures resemble the original structures. However, in comparison with the F structure, there is a certain spin density over the Br-atom.

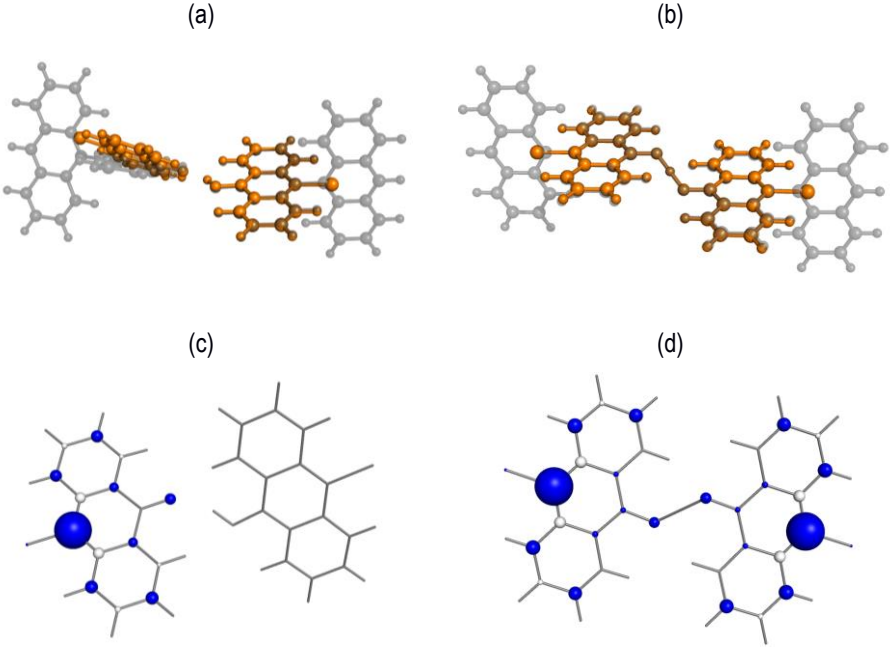

Figure 27. Overlap between (a) Br-substituted and C original anthranol/anthroxyl minima, and (b) Br-substituted D original anthranol/anthranol TS structures. Spin density distribution of Br-substituted (c) minimum and (d) TS.

SH-substituted optimized structure shows the largest anthranol/anthroxyl angle among all the substituted pairs, while the SH-substituted TS structure shows good agreement with the original TS structure (see *Figure 28*). Possibly the major activation energy of this pair, compared with the other substituted pairs, is caused by the abrupt position (dihedral C8-C1-C8'-C1' = 43.8º) showed at SH substituted optimized structure. SH-substituted optimized structure presents some spin density distributed over the sulphur atom attached to the 9 carbon, while the original structure does not present spin density over the back 9-anthracene ring.

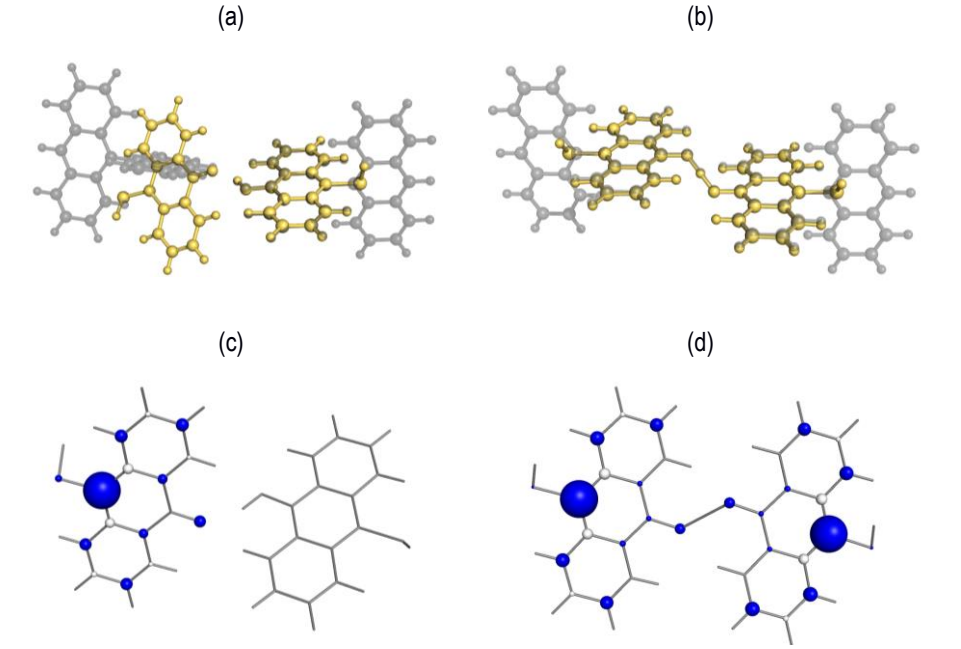

Figure 28. a) Overlap between (a) SH-substituted and C original anthranol/anthroxyl minima, and (b) SH-substituted D original anthranol/anthranol TS structures. Spin density distribution of SH-substituted (c) minimum and (d) TS.

Finally, the Methyl-TS structure varies from the TS original structure, twisting a little (dihedral C8-C1-C8'-C1' = 30.1º) between the anthranol/anthroxyl molecules (see *Figure 29*). As the other structures, the Methyl-optimized structure also forms an angle between the anthranol/anthroxyl pair (dihedral C8-C1-C8'-C1' = 37.3º). However, it does not adopt the flat shape of the CN-structure. Note that the spin density agrees with the spin density of the anthranol/anthroxyl original pair.

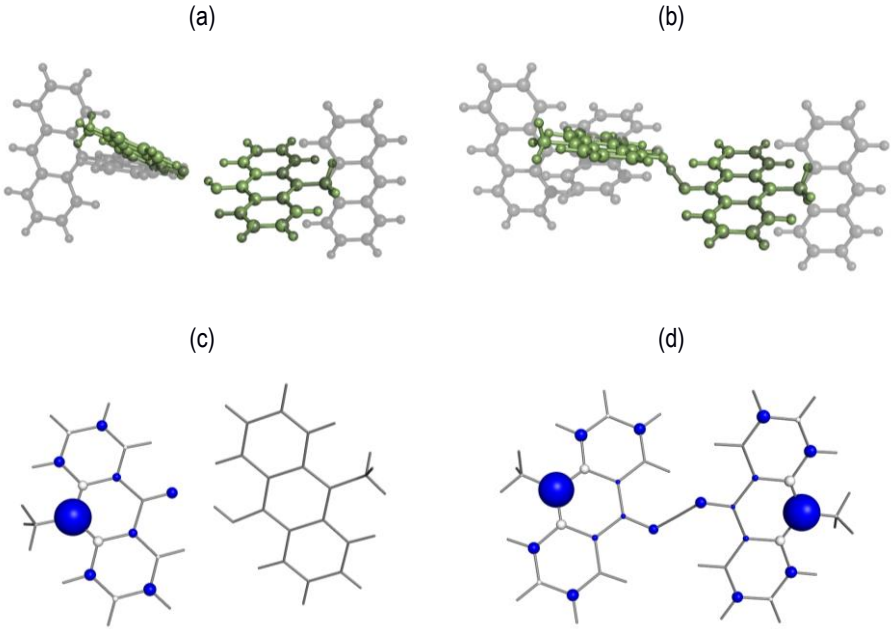

Figure 29. a) Overlap between (a) Methyl-substituted and C original anthranol/anthroxyl minima, and (b) Methyl-substituted D original anthranol/anthranol TS structures. Spin density distribution of Methyl-substituted (c) minimum and (d) TS.

The effect of the electron withdrawing and donating groups in the PCET reaction has been studied proposing some alternatives to the anthranol/anthroxyl pair. Five functional groups (-CN, -F, -Br, -SH and -Methyl) have been used to replace the back 9-anthracene.

Full optimizations and TS search calculations have been performed with each substituted anthranol/anthroxyl pair in order to study the change in the activation energy, the spin density

distribution and the geometry. While all the groups affected the activation energy of the reaction, -CN and -SH groups yielded the largest changes. The -CN group considerably reduces the activation energy, whereas the -SH group does the opposite. Spin density distribution behave similarly in all the groups except for the -CN group, that delocalizes an appreciable amount of spin density in the -CN group. This phenomenon could be the cause of the smaller activation energy of the -CN substituted pair. The geometry of the 100 K Opt structures of all the substituted pairs seems to form a wider angle (ranging from 37.0º to 44.0º) between the anthranol and anthroxyl molecules than the original Opt structure, with a value of 26.9º, being most abrupt in the -SH Opt structure, with a value of 43.8º. The geometry of the TS structures of the -F, -Br and -SH pair remains relatively unaltered compared with the original TS structure, while the -CN and -Methyl groups alter the TS structure. The -Methyl group forms forces the 2 anthracene rings to come out-of-plane in parallel planes, while the -CN group places the two semi-radicals in the same plane.

10. CONCLUSIONS

It has been possible to properly study the thermodynamical behavior of the anthranol/anthroxyl system. The TS structure and the 200 K X-Ray structure resemblance yields to think that once the energy needed for the PCET reaction to start is overcome, the phase of the crystal consists in an average structure containing all the structures of the reaction pathway. Therefore, further studies implying molecular dynamics are needed in order to properly study the statistical behavior of the system, which are out of the range of this work. While the activation energy of the anthranol/anthroxyl pair between the full optimized 100 K structure and the transition state structure is 11.11 kcal mol^{-1}, the activation energy if starting from X-Ray 100 K structure is 5.15 kcal mol^{-1}. This phenomenon, together with the similar O-O and O-H distances of both the X-Ray 100 K and full optimized 100 K structures of the anthranol/anthroxyl pair, yields to think that crystal packing of anthranol/anthroxyl solid decreases the activation energy of the PCET reaction.

Several pairs have been extracted from both 100 K and 200 K structures, to model the magnetic behavior of the solid at the two phases. Model structure and MSK approximations have been used to speed up the calculations. Only two dimers of anthranol/anthroxyl pairs presented magnetic coupling: one from the 100 K structure and its analogous for the 200 K structure. The magnetic coupling seems to appear due to the overlap of the aromatic rings of the main anthracene, and is influenced by the proximity between the aromatic rings. Accordingly, the magnetic topology at 100 K is 0D and consists in isolated AFM dimers. At 200 K, the magnetic topology becomes 1D and can be viewed as isolated AFM chains along "*a*" axis.

Two magnetic models, one for the 100 K crystal structure and another for the 200 K crystal structure, have been proposed. While the 100 K magnetic model describes correctly the magnetic behavior of the anthranol/anthroxyl solid before the phase transition, the 200 K model can only describe correctly the first stages after the phase transition. Surprisingly, the simulated gap between the values of χT at the phase transition is in agreement with experimental. The failure of the 200 K magnetic model to describe the experimental behavior at higher

temperatures could be due to the complex statistical behavior the anthranol/anthroxyl solid might present at 200 K.

The effect of the electron withdrawing and donating groups in the PCET reaction has been studied proposing some alternatives to the anthranol/anthroxyl pair. Five functional groups (-CN, -F, -Br, -SH and -Methyl) have been used to replace the back 9-anthracene. Apparently, the -CN group will favor the most the PCET reaction since considerably reduces the activation energy barrier. Certainly, the -SH group increases the activation energy and, in term, makes it more difficult for the PCET to occur.

11. REFERENCES AND NOTES

1. Y. Hirao; T. Saito; H. Kurata; T. Kubo *Angew. Chem.* **2015**, *54*, 2402 –240.
2. J. M. Mayer *Annu. Rev. Phys. Chem.*, **2004**, *90,* 55-363.
3. H. Matsuoka; J. Shen; A. Kawamori; K. Nishiyama; Y. Ohba; S. Yamauchi *J. Am. Chem. Soc.* **2011**, *133*, 4655–4660.
4. H. Eklund; U. Uhlin; M. Farnegardh ; D. T. Logan; P. Nordlund *Prog. Biophys. Mol. Biol.* **2001,** *77*, 177-268.
5. H. V. Huynh; T. J. *Chem. Rev.* **2007**, *107*, 5004-5064.
6. J. M. Mayer; D. A. Hrovat; J. L. Thomas; W. T. Borden *J. Am. Chem. Soc.*, **2002**, *124*, 11142-11147.
7. A. Sirjoosingh; S. Hammes-Schiffer *J. Phys. Chem.* **2011**, *115*, 2367–2377
8. G. A. DiLabio; E. R. *J. Am. Chem. Soc.* **2007**, *129*, 6199-203.
9. P. Hohenberg; W. *Phys. Rev*. **1964,** *136*, B864.
10. W. Kohn; L. J. Sham *Phys. Rev.* **1965,** *140*, A1133.
11. Gaussian 09, Revision A.02, M. J. Frisch; G. W. Trucks; H. B. Schlegel; G. E. Scuseria; M. A. Robb; J. R. Cheeseman; G. Scalmani; V. Barone; G. A. Petersson; H. Nakatsuji; X. Li; M. Caricato; A. Marenich; J. Bloino; B. G. Janesko; R. Gomperts; B. Mennucci; H. P. Hratchian; J. V. Ortiz; A. F. Izmaylov; J. L. Sonnenberg; D. Williams-Young; F. Ding; F. Lipparini; F. Egidi; J. Goings; B. Peng; A. Petrone; T. Henderson; D. Ranasinghe; V. G. Zakrzewski; J. Gao; N. Rega; G. Zheng; W. Liang; M. Hada; M. Ehara; K. Toyota; R. Fukuda; J. Hasegawa; M. Ishida; T. Nakajima; Y. Honda; O. Kitao; H. Nakai; T. Vreven; K. Throssell; J. A. Montgomery; Jr.; J. E. Peralta; F. Ogliaro; M. Bearpark; J. J. Heyd; E. Brothers; K. N. Kudin; V. N. Staroverov; T. Keith; R. Kobayashi; J. Normand; K. Raghavachari; A. Rendell; J. C. Burant; S. S. Iyengar; J. Tomasi; M. Cossi; J. M. Millam; M. Klene; C. Adamo; R. Cammi; J. W. Ochterski; R. L. Martin; K. Morokuma; O. Farkas; J. B. Foresman; D. J. Fox *Gaussian, Inc*., Wallingford CT, **2016**.
12. (a) A.D. Becke *Phys. Rev. A* **1988**, *38*, 3098; (b) A.D. Becke *J. Chem. Phys.* **1993**, *98*, 5648; (c) C. Lee; W. Yang; R. G. Parr *Phys. Rev. B* **1988**, *37*, 785.
13. 6-31+G(d, p) basis set: (a) P. C. Hariharan; J. A. Pople *Theor. Chem. Acc.* **1973**, *28*, 213-22. (b) M. M. Francl; W. J. Pietro; W. J. Hehre; J. S. Binkley; D. J. DeFrees; J. A. Pople; M. S. Gordon *J. Chem. Phys.* **1982,** *77*, 3654-65.
14. Firefly QC package [1], which is partially based on the GAMESS (US) [2] source code.
    13.1. A. A. Granovsky, Firefly version 8, www http://classic.chem.msu.su/gran/firefly/index.html
    13.2 M. W. Schmidt: K. K. Baldridge; J. A. Boatz; S. T. Elbert; M. S. Gordon; J. H. Jensen; S. Koseki; N. Matsunag; K. A. Nguyen; S. Su; T. L. Windus; M. Dupuis; J. A. Montgomery *J.Comput.Chem*. **1993,** *14*, 1347-1363.
15. S. Vela; F. Mota; M. Deumal; R. Suizu; Y. Shuku; A. Mizuno; K. Awaga; M. Shiga; J. J. Novoa; J. Ribas-Arino. *Nat Commun*. **2014**, *5,* 4411.
16. U. C. Singh; P. A. Kollman *J. Comp. Chem.* **1984**, *5*, 129 – 145.

12. ACRONYMS

PCET: Proton Coupled Electron Transfer

HAT: Hydrogen Atom Transfer

TS: Transition State.

DFT: Density Functional Theory

UB3LYP: Unrestricted 3-parameter formulation Becke, Lee, Yang and Parr.

MSK: Merz-Singh-Kollman

Opt: Optimized

emu: ElectroMagnetic Units

HOMO: Highest occupied molecular orbital

APPENDICES

APPENDIX 1: SPIN DENSITY DISTRIBUTION

Atom	Anthranol	Anthroxyl
PCET Hydrogen	-0.001112	
Oxygen	0.001252	0.178524
Carbon 9	0.000124	0.492431
Carbon 2	0.000508	0.166383
Carbon 7	0.000943	0.166148
Carbon 4	0.000148	0.136570
Carbon 5	0.000112	0.134556

Table I. Energy spin distribution over the X-Ray 100 K structure.

Atom	Semi-radical 2	Semi-radical 1
PCET Hydrogen	-0.006617	
Oxygen	0.068637	0.068619
Carbon 9	0.235756	0.235814
Carbon 2	0.075909	0.075892
Carbon 7	0.077213	0.077233
Carbon 4	0.068965	0.068948
Carbon 5	0.068756	0.068773

Table II. Energy spin distribution over the X-Ray 200 K structure.